ACS SyntheticBiology

Research Article

pubs.acs.org/synthbio

SYNZIP Protein Interaction Toolbox: *in Vitro* and *in Vivo* Specifications of Heterospecific Coiled-Coil Interaction Domains

Kenneth Evan Thompson,[†] Caleb J. Bashor,[‡,§,∥] Wendell A. Lim,[‡] and Amy E. Keating[†,*]

[†]Department of Biology, Massachusetts Institute of Technology, Cambridge, Massachusetts 02139, United States

[‡]Howard Hughes Medical Institute, Department of Cellular and Molecular Pharmacology and [§]Graduate Group in Biophysics, University of California San Francisco, San Francisco, California 94158, United States

Supporting Information

ABSTRACT: The synthetic biology toolkit contains a growing number of parts for regulating transcription and translation, but very few that can be used to control protein association. Here we report characterization of 22 previously published heterospecific synthetic coiled-coil peptides called SYNZIPs. We present biophysical analysis of the oligomerization states, helix orientations, and affinities of 27 SYNZIP pairs. SYNZIP pairs were also tested for interaction in two cell-based assays. In a yeast two-hybrid screen, >85% of 253 comparable interactions were consistent with prior *in vitro* measurements made using coiled-coil microarrays. In a yeast-signaling assay controlled by coiled-coil mediated scaffolding, 12 SYNZIP pairs were successfully used to down-regulate the expression of a reporter gene following treatment with α-factor. Characterization of these interaction modules dramatically increases the number of available protein interaction parts for synthetic biology and should facilitate a wide range of molecular engineering applications. Summary characteristics of 27 SYNZIP peptide pairs are reported in specification sheets available in the Supporting Information and at the SYNZIP Web site [http://keatingweb.mit.edu/SYNZIP/].

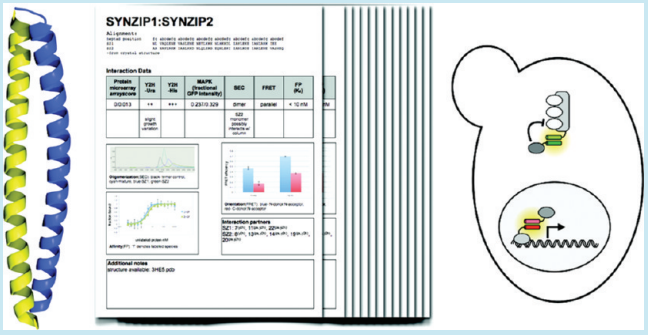

KEYWORDS: *protein−protein interaction, synthetic biology, coiled coil, heterodimer*

The central goal in synthetic biology is to engineer living systems that exhibit new behaviors and functions. The most common approach is to start with a set of standard biological parts or modules and to combine them in new ways to give rise to desired properties. To design increasingly complex systems, larger sets of characterized parts are required. Several groups have addressed the challenge of refining and standardizing biological parts and devices by assessing the activity of different promoters in cell-based transcriptional assays, designing synthetic ribosome binding sites, engineering directed transcript cleavage by RNase, creating libraries of simple logic gates, and constructing orthogonal bacterial expression systems.[1−8] These studies have generated diverse, well-defined modules, and collections of many well-characterized molecular components can be found in the Registry of Standardized Parts (http://partsregistry.org/) and at BioFAB (http://www.biofab.org/). Most of the parts currently used for biological design are directed toward regulation at the level of transcription or translation, and the set of reagents available for post-translational control is limited. A small number of protein interaction domains, including coiled coils, PDZ, SH3, and GBD domains, have been used to localize or oligomerize proteins. These have been applied in both scaffolding and signaling applications with impressive results,[9−11] but the limited number and diversity of well-characterized domains restricts the complexity that can be designed. A larger repertoire of interaction reagents could facilitate the implementation of more complex systems.

Coiled coils, structures in which α helices intertwine to form superhelical bundles, are the simplest of all protein interaction motifs and have a rich history of use in molecular engineering. Coiled coils of only ∼20−50 residues can fold and oligomerize into homo- or heteromeric 2-to-4 helix bundles,[12] and many of the sequence features that govern coiled-coil interaction specificity are known.[13−15] Coiled-coil sequences have a repeating seven-residue pattern, termed a heptad repeat, that is denoted $(abcdefg)_n$. Hydrophobic residues occupy many of the *a* and *d* positions, forming a well packed interface, and *e* and *g* positions on opposing helices tend to be electrostatically complementary. Homodimerizing coiled coils have been used to stabilize complexes,[16−20] study self-assembly,[21] and dimerize artificial transcription factors.[22−24] Beyond using protein interactions for self-oligomerization, heterodimerizing coiled coils allow the creation of more complex systems by bringing different components together. Recent studies have applied coiled-coil heterodimers to nanofiber formation[25−27] three-dimensional organization of nanoscale particles,[28] the engineer-

Received: October 25, 2011
Published: February 2, 2012

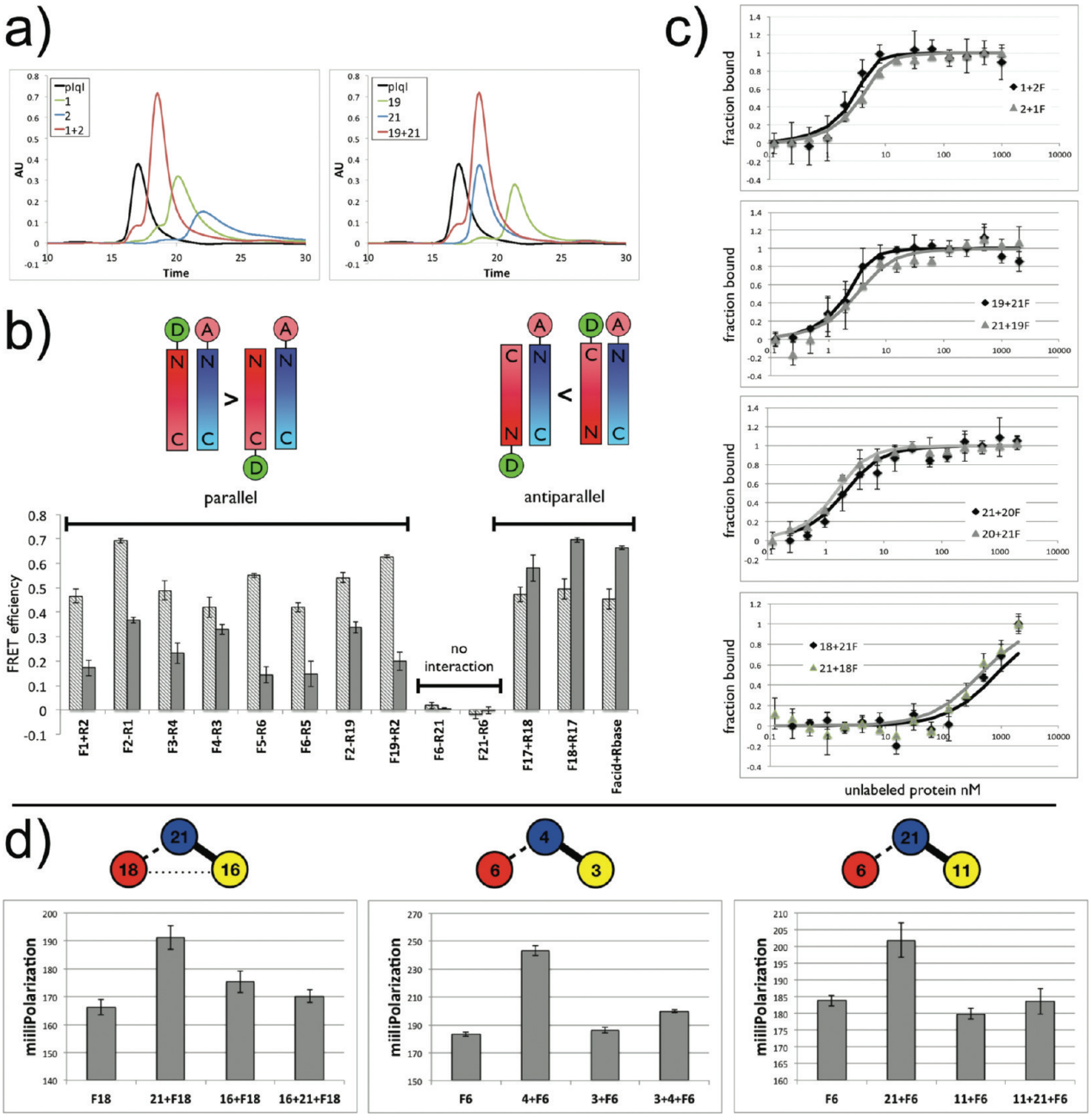

Figure 1. Biophysical properties of SYNZIPs. (a) SEC elution traces. The left panel shows SYNZIP1 in green, SYNZIP2 in blue, the SYNZIP1:SYNZIP2 mixture in red, and the GCN4-pIqI trimer control in black. The right panel shows SYNZIP21 in blue, SYNZIP19 in green, the SYNZIP19:SYNZIP21 mixture in red, and the GCN4-pIqI trimer control in black. (b) The cartoon shows a schematic of the FRET assay, and the bar graph shows FRET efficiencies for selected pairs. Hatched bars are the N-terminal donor/N-terminal acceptor mixes, and gray bars are the C-terminal donor/N-terminal acceptor mixes. (c) Representative FP titrations plotted as the fraction of the fluorescein labeled protein bound. Each plot shows reciprocal measurements, with each interaction partner used in turn as the labeled species. Raw data, showing millipolarization, is available in Supplementary Figure 3. (d) Competition between strong and weak SYNZIP pairs. Observed interactions are summarized in graphs at the top of each plot, where circles represent SYNZIPs, bold lines indicate strong interactions, and dotted lines indicate weak interactions observed in this assay. The fluorescence polarization of different mixtures is shown in the bar graphs. "F" and "R" in the legend of each plot designates the species labeled with fluorescein or rhodamine, and the curves show the best fit to the data (see Methods). Error bars show ±1 SD over three (b and c) or four (d) replicates.

ing of protein-based hydrogels,[29] and signaling pathway modulation *via* recruitment of kinases/phosphatases.[9] These studies indicate there is a promising future in using coiled-coil reagents in biomolecular engineering, one limitation being the small number of interacting partners to choose from.

Reinke *et al.* recently reported a set of 23 synthetic heteroassociating coiled coils called SYNZIPs.[30] The SYNZIPs were originally designed to interact heterospecifically with the leucine-zipper regions of human bZIP transcription factors as parallel coiled-coil dimers and in this context were referred to as anti-bZIPs.[31] Following assessment of the interaction of the anti-bZIPs with their human protein targets,[31] the designed proteins were tested for pairwise interactions among themselves using a coiled-coil microarray assay.[30] Twenty-three peptides

dx.doi.org/10.1021/sb200015u | *ACS Synth. Biol.* 2012, 1, 118–129

Table 1. SYNZIP Pair Biophysical Properties

SYNZIP	interaction[a]	oligomerization[b]	orientation[c]	av K_d[d]
1	off	monomer	n/a	n/a
2	off	monomer	n/a	n/a
3	off	monomer	n/a	n/a
4	off	monomer	n/a	n/a
5	off	monomer	n/a	n/a
6	off	monomer	n/a	n/a
11	off	monomer	n/a	n/a
14	self-interaction	dimer	not determined	inconclusive
16	self-interaction	dimer	not determined	inconclusive
17	off	inconclusive	n/a	n/a
18	off	monomer	n/a	n/a
19	off	monomer	n/a	n/a
20	self-interaction	dimer	not determined	inconclusive
21	self-interaction	dimer	not determined	inconclusive
1 + 2	on	dimer	parallel	<10
2 + 14	on	dimer	parallel	<10
2 + 19	on	dimer	parallel	<10
2 + 20	on	dimer	parallel	<10
3 + 4	on	dimer	parallel	<30
3 + 5	weak	no interaction	n/a	>400[e]
4 + 6	weak	no interaction	n/a	>400[e]
4 + 21	on	dimer	parallel	<10
5 + 6	on	dimer	parallel	<15
5 + 16	on	dimer	parallel	<10
5 + 18	weak	no interaction	n/a	>200[e]
5 + 21	on	dimer	parallel	<10
6 + 19	on	dimer	parallel	<10
6 + 20	on	dimer[f]	parallel	<10
6 + 21	weak	multiple species	n/a	>200[e]
11 + 18	off	no interaction	n/a	not determined
11 + 19	on	dimer	parallel	<10
11 + 20	on	dimer	parallel	<10
11 + 21	on	dimer[f]	parallel	<10
14 + 17	on	dimer	parallel	<10
14 + 21	on	dimer[g]	parallel	<10
16 + 19	on	dimer	parallel	<10
16 + 20	on	dimer[g]	parallel	<10
16 + 21	on	dimer[g]	parallel	<10
17 + 18	on	dimer	antiparallel	<10
17 + 21	on	dimer	parallel	<10
18 + 19	on	dimer	parallel	<10
18 + 20	on	dimer	parallel	<15
18 + 21	weak	no interaction	n/a	>300[e]
19 + 20	off	not tested	n/a	not detected
19 + 21	on	dimer	parallel	<10
20 + 21	on	dimer[g]	parallel	<10

[a]Determined from the SEC, FRET, and FP data. [b]Determined by SEC. [c]Determined by FRET. [d]From best fit, or average of the two best-fit K_d values when each species was labeled for the assay. [e]No upper baseline was obtained in the assay. [f]Elution trace with a leading edge slightly larger than dimer. [g]Mixture of two homo-oligomerizing species.

were selected as potentially useful heteroassociating interaction modules on the basis of minimal self-interaction and strong heteroassociation with one or more of the other designs. These 23 anti-bZIP peptides were renamed SYNZIPs. Comprehensive analysis of pairwise SYNZIP interactions revealed many interesting network patterns, such as orthogonal interaction pairs and hub-spoke motifs. Crystallographic studies of 2 of the interacting pairs, SYNZIP1:SYNZIP2 and SYNZIP5:SYNZIP6, demonstrated that these form parallel, dimeric coiled coils.[30]

Although *in vitro* array studies have established that many SYNZIP pairs form tight, heterospecific complexes, more information about their interaction properties is required if they are to be employed as standard molecular interaction parts. Furthermore, SYNZIP interactions have yet to be validated inside cells. To facilitate the use of these modules for diverse purposes, we here present extensive biophysical characterization of numerous SYNZIP interactions *in vitro* and report the ability of many pairs to interact with the anticipated specificity in yeast.

RESULTS AND DISCUSSION

Maximal utility of the SYNZIPs, for applications in molecular engineering, demands knowledge of their interaction geometries and affinities. Although the SYNZIPs share many sequence features in common with bZIP leucine zippers, which form parallel coiled-coil dimers to allow the transcription factors to bind DNA, it has also been observed that even a single amino-acid change can alter the oligomerization state or helix orientation of coiled coils.[32−34] Crystal structures of two SYNZIP complexes revealed that these form parallel heterodimers, and Reinke *et al.* further argued that many other SYNZIP pairs are likely to do so.[30] However, establishing this experimentally requires extensive biophysical characterization, which we report here.

For synthetic biology applications, SYNZIPs must form the expected interactions in cells when fused to a variety of domains. To test whether SYNZIPs expressed as fusion proteins can interact similarly to shorter coiled-coil peptides, we carried out *in vitro* studies using MBP fusions. We chose 14 SYNZIPs for *in vitro* testing, selecting proteins that had many interaction partners in the prior coiled-coil microarray tests or that interacted with a SYNZIP that had many interaction partners. We also tested SYNZIP fusions for function in cells, assaying 22 SYNZIPs as Gal4 DNA-binding and activation-domain constructs in a two-hybrid screen and 14 SYNZIPs as Msg5- and Ste5-fusions in a MAPK signaling assay.

SYNZIP Oligomerization State. Oligomerization state is a critical parameter for interaction reagents. For example, it was recently demonstrated that varying the number of protein interaction sites on a synthetic scaffold can tune the output of synthetic metabolic pathways.[10,11] Thus, we developed a moderate-throughput strategy to assess the oligomerization state of numerous SYNZIPs and SYNZIP complexes.

SYNZIPs have a molecular weight of ∼5 kDa, which is one of their advantages as interaction modules. Their small size precludes easy determination of oligomer state using size exclusion chromatography (SEC), but using MBP fusion proteins allowed us to separate oligomers based on molecular weight changes of ∼50 kDa, which corresponds to a significant difference in hydrodynamic radius. Interacting SYNZIP-MBP fusions are composed of two globular domains attached to a rigid coiled-coil linker, and this unusual shape could potentially influence their elution profiles. Thus, we used the SYNZIP1:SYNZIP2 heterodimer with each peptide fused to MBP as a dimer standard[31] and made a homotrimeric mutant of the yeast bZIP GCN4, GCN4-pIqI[35] fused to MBP as a trimer standard.

SEC results for SYNZIP1:SYNZIP2 and SYNZIP19:SYNZIP21 are shown in Figure 1a, and results for all other tested pairs are summarized in Table 1 and detailed in the Supporting Information. The majority of individual SYNZIPs eluted as monomers, as expected in the absence of a heterodimerization partner, but there were exceptions. Several constructs eluted later than most monomers and/or had asymmetric tailing peaks (Figure 1a, Supplementary Data 1). It is not unexpected that SYNZIP monomers would have some affinity for the column matrix, as leucine-zipper monomers are mostly unfolded and expose many hydrophobic residues. The degree of residual structure in SYNZIP monomers could also vary with sequence. Several zippers that appeared to form homo-oligomers at 10 μM injection concentrations were further tested for self-association using fluorescence polarization at lower concentrations (see below).

In cases where the individual zippers eluted as monomers, it was very clear when a dimer formed upon mixing because there was a shift of almost all protein to a dimer peak. For example, in Figure 1a, the left panel shows the elution profiles of SYNZIPs 1 and 2. SYNZIP1 eluted primarily in a peak at the size expected for a monomer. Most of SYNZIP2 eluted slightly later than observed for other monomers. The SYNZIP1:SYNZIP2 mixture gave a strong peak in the dimer size range. SEC could also be used to detect cases where a monomeric species was mixed with a homo-oligomerizing partner, forming a preferential heterodimer. For example, SYNZIP21 alone eluted as a dimer, and SYNZIP19 eluted later than most monomers. It was nevertheless clear that a dimeric complex was formed by the mixture, because monomeric species all but disappeared from the elution profile and instead most of the protein eluted in the dimer-size peak (Figure 1a, right panel). When two homodimerizing SYNZIPs were mixed and gave a large peak at the expected dimer elution volume, the SEC data could not be used to confirm interaction. Nevertheless, such experiments supported the formation of dimers rather than higher order species, and pairs showing this behavior (*e.g.*, SYNZIP14:SYNZIP21, Supplementary Data 1) were further characterized using orientation and affinity assays (Table 1).

SYNZIP Interaction Orientation. Although certain sequence features suggest a parallel arrangement of SYNZIP helices,[30] we sought to confirm this experimentally because knowing the interaction geometry can be critical for molecular engineering. For example, knowledge of helix orientation was necessary in the design of artificial transcription factors using coiled coils fused to DNA binding domains, as demonstrated with zinc fingers[23] and polyamides.[24]

To determine the interaction orientation of SYNZIP helices, we employed a FRET assay in which the first partner was labeled with a fluorescein donor on either the N- or C-terminus, and the second partner was N-terminally labeled with a rhodamine acceptor (Figure 1b). In a parallel complex, an N-terminal fluorescein will exhibit greater FRET efficiency than a C-terminal fluorescein when transferring energy to a rhodamine acceptor conjugated to the N-terminus of an interaction partner. An antiparallel interaction would exhibit greater FRET efficiency when a C-terminal fluoresceinated peptide was mixed with an N-terminal acceptor. Because this is a population assay, it reports only the prevailing helix orientation, and thus it is possible that mixtures of orientations are present in some cases. The crystal structures of the SYNZIP1:SYNZIP2 and SYNZIP5:SYNZIP6 pairs confirm a parallel orientation for these complexes, so these were used as parallel controls. The coiled-coil Acid-a1/Base-a1 was used as an antiparallel control[34] (Figure 1b).

For all but one of the SYNZIP interactions measured, we observed a greater FRET efficiency for the N-donor/N-acceptor mix than for the C-donor/N-acceptor mix, supporting a predominantly parallel helix orientation (Table 1). This was true regardless of which peptide was labeled with fluorescein and which was labeled with rhodamine; each complex was tested using both combinations (Supplementary Data 1). When we tested the SYNZIP6:SYNZIP21 pair that did not interact on the peptide microarrays or by SEC, no FRET signal was observed. Figure 1B shows differences in FRET efficiencies for 4 parallel SYNZIP pairs. SYNZIP17:SYNZIP18 gave the opposite pattern, indicating an antiparallel interaction similar to the antiparallel control pair Acid-a1/Base-a1 (denoted Facid + Rbase in Figure 1b). This pair eluted as a dimer in SEC,

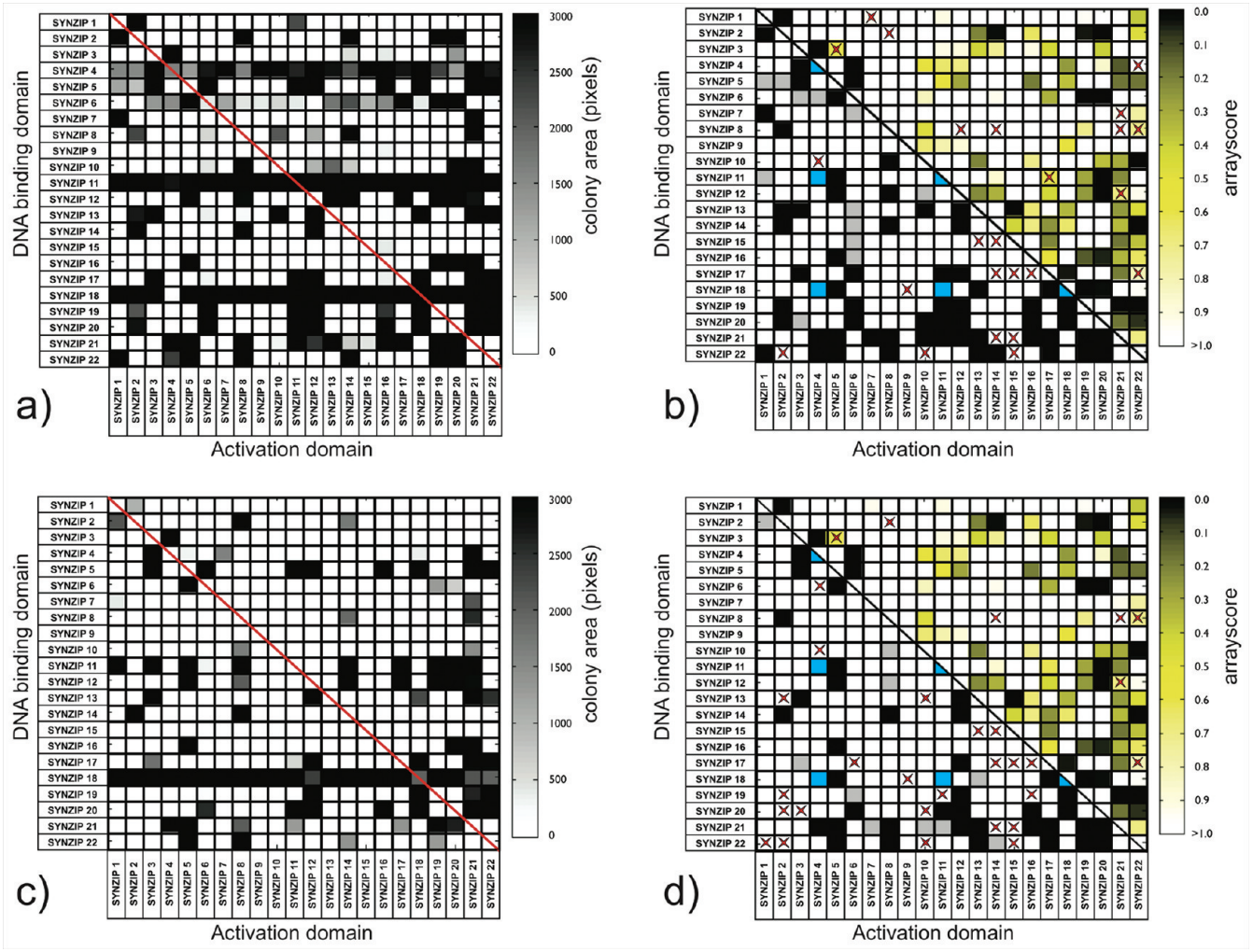

Figure 2. SYNZIP interactions detected by Y2H. (a) Histidine selection with 100 mM 3-AT, 12 days growth, represented in greyscale with white as no growth and black as strongest growth. (b) Heat map comparing Y2H data with coiled-coil microarray data, with Y2H in the lower left and microarray in the upper right. Red X's indicate an interaction observed in Y2H but not seen on the microarray or *vice versa*. Y2H data is shown as black, strong interaction; gray, undetermined interaction; white, no interaction; blue, two autoactivators (see Methods). Microarray data is the maximum of the two reciprocal measurements ranging from no interaction (white, *arrayscore* > 1) to strong interaction (black, *arrayscore* = 0).[30] (c, d) Uracil selection, 12 days growth and heat map comparison with microarray, as in panel b.

indicating the structure is likely that of an antiparallel heterodimer. Manual inspection of the sequences of SYNZIPs 17 and 18, as they would interact in an antiparallel heterodimer, suggests two possible alignments that maximize the helix−helix overlap and predict electrostatic complementary at adjacent interfacial *e* and *g* positions (Supplementary Data 1).

SYNZIP Interaction Affinities. Knowledge of the affinities of SYNZIP complexes is necessary for determining the concentration range at which they will be effective interaction reagents. It has also been demonstrated that changing the affinity of a coiled-coil interaction in a MAPK signaling assay can tune the effect of a modulator and create complex pathway responses.[9] We assayed 27 SYNZIP pairs using a fluorescence polarization (FP) assay in which fluoresceinated MBP-fusion SYNZIP was mixed with increasing concentrations of an unlabeled MBP-fusion partner.

The majority of SYNZIP interacting pairs tested were very stable, with dissociation constants less than 10 nM (Figure 1). Quantifying affinities tighter than this is beyond the sensitivity of the assay. Thus the reported K_d values for tight binders can be considered an upper limit. Overall, the affinity data agree well with data from other assays. Strong hetero interactions detected in the previous coiled-coil array study[30] and by SEC all had very tight affinities as measured by FP. For weakly interacting pairs, *i.e.*, those not previously observed to interact and those that interacted only weakly on protein microarrays, interactions were observed only at higher concentrations, if at all, and we could not detect an upper baseline even at concentrations approaching 20 μM (Supplementary Data 1 and Figure 1). Finally, most of the self-interactions originally detected by SEC exhibited a slow increase in polarization with increasing concentration, inconsistent with cooperative two-state binding (Supplementary Figure 2). Figure 1c shows titration binding curves for three tight SYNZIP interactions and one weak interaction.

We also tested whether a tight pair could compete effectively with a weak pair. For example, the SYNZIP18:SYNZIP21 pair showed no signal on the coiled-coil microarrays[30] and showed weak interaction in FP studies (K_d > 250 nM). When SYNZIP18 labeled with fluorescein was mixed with a high concentration of SYNZIP21, we detected an interaction between the two as indicated by an increase in polarization.

dx.doi.org/10.1021/sb200015u | *ACS Synth. Biol.* 2012, 1, 118−129

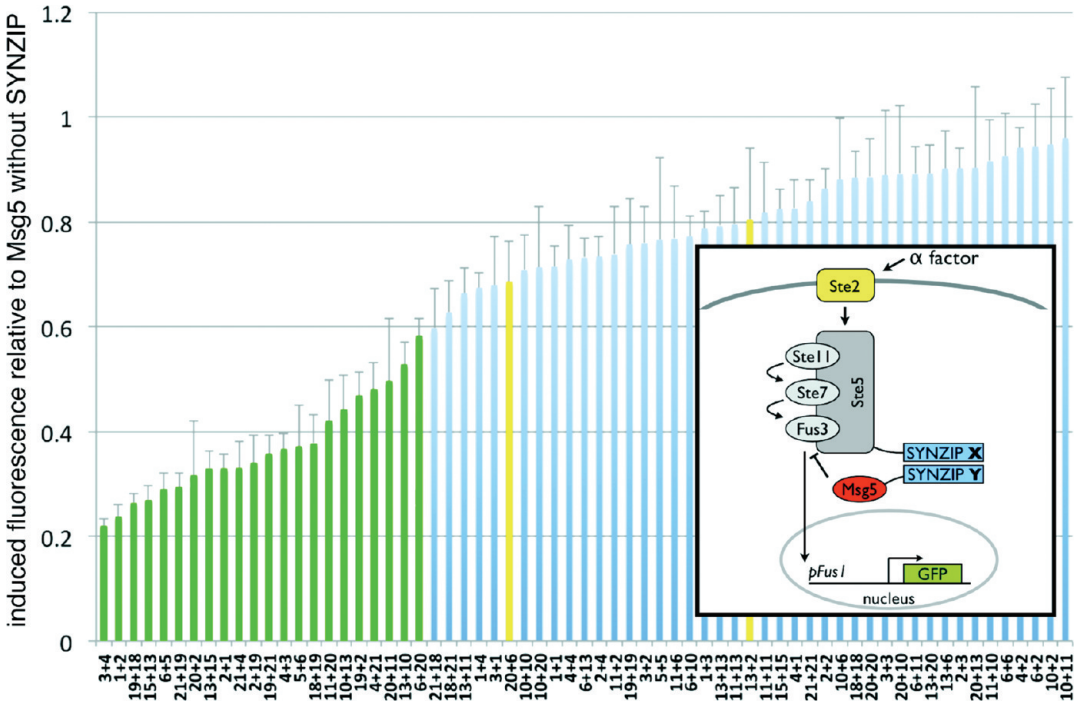

Figure 3. Cell fluorescence as a measure of MAPK pathway modulation by SYNZIP pairs. SYNZIP pairs are rank ordered, left-to-right, by the relative mean cell fluorescence induced when the pair was used to recruit Msg5 to Ste5 (inset). The first SYNZIP listed was fused to the Ste5 scaffold protein and the second was fused to Msg5 phosphatase. Green bars indicate interacting pairs as determined by Y2H and coiled-coil microarray. Two instances where SYNZIPs that interacted on the array showed little MAPK pathway down-regulation are highlighted in yellow. Average signals from 4 replicates are reported relative to the average signal for a Ste5-SYNZIPX:Msg5-nozipper control, with X the corresponding SYNZIP for the Ste5 fusion. Error bars show 1 SD of 4 measurements.

However, when a high concentration of SYNZIP16, which forms a tight complex with SYNZIP21, was included in the mixture, the weak interaction no longer occurred (Figure 1d). Similar trends were observed for other pairs, as shown in Figure 1d.

SYNZIP Interactions in a Yeast Two-Hybrid Assay. The yeast two-hybrid (Y2H) assay provides a straightforward and widely used way to assess the ability of SYNZIPs to mediate protein association in cells.[36−39] The proteins to be tested are individually fused to the DNA-binding (bait) and activation domains (prey) of the Gal4 transcription factor. In our version of the assay, a SYNZIP−SYNZIP interaction reconstitutes the transcription factor, which then drives expression of *URA3* and *HIS3* reporter genes. A positive readout requires that the fusion proteins be expressed, localize to the nuclei of living cells, and interact. Thus, Y2H can be used to determine whether SYNZIP fusions are toxic to cells, and whether concentrating them in the nucleus affects their interaction behavior.

We tested all pairwise combinations of 22 SYNZIPs both as DNA-binding and activation domain fusions for both selection assays. Figure 2a and c summarizes our observations that many SYNZIP pairs did not support growth, as expected, and that rapidly growing colonies were often detected reciprocally in both fusion contexts. For all of the SYNZIPs in each fusion context, we observed comparable growth rates on selection media for plasmid maintenance only, indicating that constitutive expression of these SYNZIP fusion constructs had no noticeable effect on cell viability. There were 3 autoactivating DNA-binding domain fusions (SYNZIPs 4, 11 and 18) that permitted growth alone and regardless of partner. We did not observe any autoactivating activation-domain fusions, indicating that the SYNZIPs did not directly bind the promoters of the reporters in this system. The Y2H assay showed good overall agreement with interaction profiles observed in previous work using coiled-coil microarrays.[30] On the basis of comparisons of 235 pairs (see Methods) under -histidine selection, 12 strong interactions observed by Y2H were not seen on the arrays and 12 strong array interactions were not detected by Y2H, for an overall discrepancy of ∼10% (Figure 2b). The -uracil selection data allowed us to compare 237 pairs, and we found that 7 strong interactions observed by Y2H were not seen on the arrays, and 23 strong array interactions were not detected by Y2H, for an overall discrepancy of ∼13% (Figure 2d). We observed several interactions involving SYNZIP8 that were not detected in the original study, including pairs 8:2, 8:14, and 8:21. We also did not see a previously strong interaction between SYNZIPs 13 and 15, although this interaction was detected in the MAPK assay described below. These results indicate that many of the SYNZIP pairs can function as general interaction reagents in a yeast nuclear context. The full data sets are available in Supplementary Data 3.

Repressing Yeast α-Factor Response Using SYNZIPs as Recruitment Domains for a Negative Pathway Modulator. Bashor *et al.* recently demonstrated how the output of the yeast mating pathway can be modulated by recruiting kinases or phosphatases to the protein scaffold Ste5 in the yeast cytoplasm.[9] A heterodimeric variant of a native bZIP protein dimerization domain was used in the original application.[15] In our version of this assay, one SYNZIP was fused to the Ste5 scaffold to provide a binding site for a second SYNZIP that was fused to the phosphatase Msg5 (Figure 3, inset). The effect of recruiting Msg5 to Ste5 on the mating response was detected using a GFP reporter gene. Following α-factor induction of the MAPK signaling cascade, we expected

dx.doi.org/10.1021/sb200015u | *ACS Synth. Biol.* 2012, 1, 118−129

SYNZIP1:SYNZIP2

Alignment:

```
heptad position     fg abcdefg abcdefg abcdefg abcdefg abcdefg abcdefg abcdef
SZ1                 NL VAQLENE VASLENE NETLKKK NLHKKDL IAYLEKE IANLRKK IEE
SZ2                 AR NAYLRKK IARLKKD NLQLERD EQNLEKI IANLRDE IARLENE VASHEQ
-from crystal structure
```

Interaction Data

Protein microarray *arrayscore*	Y2H -Ura	Y2H -His	MAPK (fractional GFP intensity)	SEC	FRET	FP (K_d)
0/0.013	++	+++	0.237/0.329	dimer	parallel	< 10 nM
	slight growth variation			SZ2 monomer possibly interacts w/ column		

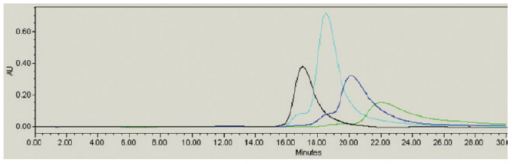

Oligomerization(SEC): black- trimer control, cyan-mixture, blue-SZ1, green-SZ2

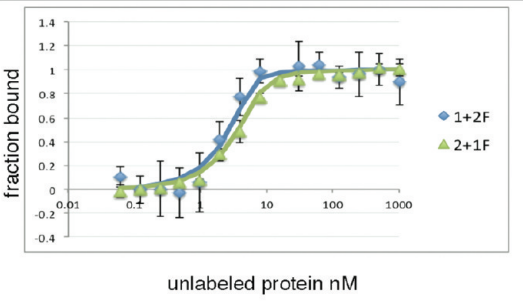

Affinity(FP): "f" denotes labeled species

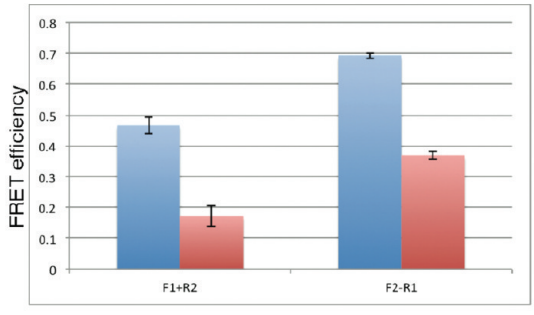

Orientation(FRET): blue- N-donor:N-acceptor, red- C-donor:N-acceptor

Interaction partners

SZ1: 7(y2h), 11(pa,y2h), 22(pa,y2h)

SZ2: 8(y2h), 13(pa,y2h), 14(pa,y2h), 19(pa,y2h), 20(pa,y2h)

Additional notes

structure available: 3HE5.pdb

Figure 4. SYNZIP interaction specification sheet for pair SYNZIP1:SYNZIP2.

that an interacting SYNZIP pair would result in reduced reporter activation compared to a control in which Msg5 was not fused to any SYNZIP. We tested 13 pairs expected to interact and 29 pairs expected not to interact on the basis of prior studies.

Figure 3 shows the normalized mean fluorescence intensity of GFP in cells 120 min after α-factor induction (raw data available in Supplementary Data 4). Tested pairs are ordered from those that gave the lowest GFP expression, at left, to those that gave the highest GFP expression at right. Those pairs observed to interact on coiled-coil microarrays are show in green, and these gave the most reduced pathway outputs, as expected. Two exceptions where expected interactions did not lead to transcriptional down-regulation are shown in yellow. For example, the SYNZIP2:SYNZIP13 interaction was very strong on the coiled-coil arrays and in the Y2H -histidine

dx.doi.org/10.1021/sb200015u | *ACS Synth. Biol.* 2012, 1, 118–129

selection, but weak in this scaffolding assay. We also observed that in one fusion context the SYNZIP6:SYNZIP20 pair, a strong interaction in our other assays, had less effect than some of the weak or undetected pairs. Weak SYNZIP pairs and self-interactions, shown in blue, had less effect on pathway output than tight pairs, as expected. The SYNZIP18:SYNZIP21 pair gave a moderate response in the scaffolding assay, although it was not detected using microarrays, in Y2H or by SEC, and gave a K_d of >250 nM by the FP assay (Supplementary Data 1). The few differences in activity observed between the scaffolding assay and Y2H are not unexpected, as the interactions are being tested in different cellular environments and at different concentrations. Overall, the MAPK signaling data indicate that many SYNZIPs can interact in a cytosolic environment, with low to moderate expression levels, while maintaining the specificity of the interactions.

SYNZIP Specification Sheets. Multifaceted characterization of SYNZIP interactions has allowed us to compile detailed biological specification sheets for 27 SYNZIP pairs (Supplementary Data 1). Figure 4 shows a specification sheet for the SYNZIP1:SYNZIP2 pair. For this pair, we present the sequence alignment of the interaction based on the crystal structure, although in most cases we present a probable alignment based on electrostatic complementary at $e-g'$ positions and other specificity determinants such Asn-Asn pairing at a-a' positions[40] (primes indicate a position on the opposite helix). Next, a table summarizes all of the interaction data we collected, including experimental observations and additional comments. The original protein microarray data are presented using *arrayscore* values, as defined in ref 30, where numbers approaching zero indicate strong binding. Yeast two-hybrid data are reported qualitatively, and increasing numbers of "+" symbols indicate larger yeast colonies for interacting SYNZIP pairs. Instances of non-reciprocal interactions with respect to DNA-binding *versus* activation-domain fusions and instances of autoactivation are noted. The α-factor MAPK repression is reported as the fractional repression of pathway output in each fusion context. The coiled-coil oligomerization state, helix orientation, and K_d based on the SEC, FRET, and FP assays are reported, with notes advising of any deviations from ideal behavior in the assays. We also present data for the biophysical assays, interactions with other SYNZIPs detected in any assays, constructs that are available, any associated PDB codes, and other comments. The SYNZIP specification sheets are intended to facilitate use of these reagents in a variety of molecular engineering applications.

Discussion. Several properties of the SYNZIPs suggest they will find utility as reagents in synthetic biology, nanotechnology, and other fields. First, the SYNZIPs predominately form high-affinity dimers, indicating they can be used for the stoichiometic assembly of fusion partners. Recent reports describe several orthogonal protein interaction domains that can be used for multiple recruitments events; however there is a limitation in the number of such pairs available. Furthermore, the affinities of the several common reagents in use, PDZ, SH3, and GBD domains, are in the upper nanomolar to lower micromolar range.[10,11] SYNZIPs could provide additional orthogonal interaction pairs, but with much higher affinity, allowing recruitment at lower expression levels. Next, for all but one of the tested pairs, our assays indicate that parallel assemblies are forming, providing a common structure for modular design. At the same time, the one instance of an antiparallel coiled coil (SYNZIP17:18) could also be useful; we are exploring the design of additional antiparallel components. Finally, tight and weak pairs have large affinity gaps and high heterospecificity. Affinity differences could allow competitive displacement strategies, where a weakly interacting partner is displaced by a stronger one, as shown in several examples in Figure 1d. Although we have only put an upper bound on the K_d's of most interacting SYNZIP pairs, there are likely to be differences among these affinities, and competitive displacement may be possible in this regime as well. Alternatively, overexpression of one partner with respect to another could lead to partner switching. Characterizing the kinetics of exchange in future work will be important for developing displacement as a design feature.

A unique feature of the SYNZIPS, compared to interaction modules such as PDZ, SH3, and GBD domains, is that they can form combinatorial pairwise interactions and thus provide access to rich sets of network motifs. To facilitate visualization and selection of such motifs, we have provided several interaction data sets in a format easily readable by Cytoscape,[41] including two sets of yeast two-hybrid data (using 2 different reporters) and the protein microarray *arrayscores* from the previously published work (Supplementary Data 5). Here we discuss several sets of the best characterized SYNZIPs that can be used to construct interesting and potentially useful network motifs.

Linear Interactions: SYNZIPs 2:19:21:4. One type of interaction network that we see among the SYNZIPs has a linear topology (Figure 5a). In this type of motif, two

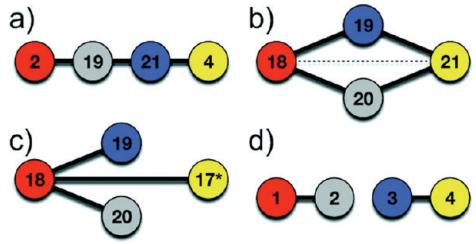

Figure 5. Network motifs constructed from SYNZIP pair interactions: (a) linear, (b) ring, (c) hub, and (d) orthogonal-pair motifs. Proteins are denoted as circles, with the SYNZIP number indicated. Strong interactions are shown with solid lines, and weak interactions with dashed lines. SYNZIPs that are not connected by an edge did not interact in the Y2H or previous coiled-coil microarray assays. All interactions and some non-interactions were confirmed *in vitro* in this work. The asterisk indicates an antiparallel interaction between SYNZIP17 and SYNZIP18.

interacting pairs (2:19 and 21:4) share an interaction between them (19:21). Although these interactions are very tight, one could imagine their use in competition experiments using stoichiometric variations. For example, a desired final state of an interaction between 2 and 19 could be inhibited by a higher amount of 21 sequestering 19. The interactions could then be switched in the presence of an excess of 4, which would bind 21, thus freeing 19 and allowing the desired final state. The off rates for several leucine zippers are in the range 10^{-2} to 10^{-4} s^{-1}, indicating that such a competition strategy could be reasonable.[42−44]

Ring Interactions: SYNZIPs 18:19:21:20. A second type of interaction network has a ring topology (Figure 5b). This motif has strong interactions among 4 SYNZIPs that make up the perimeter of a ring, with a much lower affinity interaction between 18 and 21 and no interaction observed between 19

dx.doi.org/10.1021/sb200015u | *ACS Synth. Biol.* 2012, 1, 118−129

and 20. *In vitro* data indicate that in the presence of other tight-binding partners, cross-reactivity of 18 and 21 is minimized (Figure 1d). This type of interaction could be used in a single-SYNZIP recruitment/single-SYNZIP competition arrangement, *i.e.*, SYNZIP19 could be used to recruit both 18 and 21, and overexpression of SYNZIP20 would competitively eliminate both interactions with 19.

Hub Interactions: SYNZIPs 17:18:19:20. A hub interaction motif can be formed by removing SYNZIP21 from the previously described ring motif and adding SYNZIP17 (Figure 5c). An interesting property of this interaction set is the inclusion of an antiparallel partner. One could imagine an application of this motif as a way to localize several proteins, using just one recruitment domain. For example, the hub partner 18 could be fused to a cellular membrane protein that is expressed at high levels. If expressed at lower levels, the remaining SYNZIPs could all be localized to the membrane.

Orthogonal Interactions: SYNZIPs 1:2, 3:4. Finally, the lack of interactions among several SYNZIPs provides orthogonal pair motifs (Figure 5d). These interactions allow multiple interaction events to be insulated from each other. Many applications for this type of motif can be envisioned, *e.g.*, partners from multiple orthogonal pairs could be linked together and used as a fully synthetic scaffold, or multiple pathways could be modulated by recruitment events with minimal crosstalk.

We would like to emphasize that these network motifs are inferred from interactions tested in 2-component mixtures. With some exceptions, we have not confirmed that the expected dimers are the primary species that form in solution when multiple SYNZIPs are mixed. For example, it is possible that in some combinations more than two SYNZIPs assemble into higher order complexes. Reinke *et al.* showed that 4-component mixtures (of SYNZIPs 1, 2, 3, and 4 or SYNZIPs 1, 2, 5, and 6) formed the expected pairs, implementing the orthogonal pair-type motif shown in Figure 5d. Here we have demonstrated that in several three-component mixtures, the strong interaction forms preferentially over the weak interaction (Figure 1d). It is likely, given the dimer-like sequence characteristics of the SYNZIPs, that other SYNZIPs will form the expected heterodimers even in complex mixtures, but for the majority of cases this remains to be experimentally verified.

In summary, the SYNZIPs comprise a large set of well-characterized synthetic protein interaction reagents. SYNZIPs have properties that make them well suited for use in the design of biological systems. They form highly specific, high affinity interactions, allowing them to mediate interactions at low concentrations. They are small, between 30 and 50 residues, and should incur a small metabolic cost for the cells in which they are used. Fusion proteins that we have made to SYNZIPs are soluble and well behaved *in vitro*, and cell toxicity in *E. coli* and yeast appears to be limited. Finally, SYNZIPs participate in diverse interaction motifs, providing access to complex connectivities that go beyond simple one-to-one interactions. With the extensive biophysical characterization and yeast-cell validation presented here, the SYNZIP interaction reagents greatly increase the number of available protein−protein interaction tools for scientists to use for engineering systems at the post-translational level.

METHODS

Cloning, Purification, and Dye Labeling. Synthetic genes encoding SYNZIPs with stop codons[30] were initially PCR-amplified and ligated into pENTR vectors using D-TOPO cloning (Invitrogen). Subsequent addition of N- or C-terminal Cys-Gly residues and removal of stop codons was done by PCR mutagenesis using the initial pENTR-SYNZIP vectors. SYNZIPs were then recombined into appropriate destination vectors using LR Clonase II (Invitrogen) in 5 or 2.5 μL reactions (see Supplementary Figure 4 and Supplementary Table 1 for constructs). Synthetic genes used for the MAPK assay were designed with yeast optimized codons using Gene Designer,[45] synthesized by PCR and then cloned into vectors using standard digestion and ligation procedures. For protein expression, SYNZIPs bearing N- or C-terminal Cys residues were recombined into a pMAL (NEB) derivative vector including a TEV protease cleavage site (not used) between maltose binding protein (MBP) and the Gateway linker region, and a C-terminal His6X. These destination vectors were transformed into BL21(DE3) cells (Agilent). Liquid cultures (500 mL) were induced with 1 mM IPTG at OD_{600} 0.6 for 4 h at 37 °C. Cells were pelleted, resuspended, and then lysed by sonication, and proteins were purified from the supernatant using NiNTA agarose (Qiagen) under native conditions. There was little variation in growth rate or peptide yield among different SYNZIPs, indicating overexpression of these fusion constructs did not have noticeably adverse effects on the cells. NiNTA-purified proteins were dialyzed and concentrated into PBS (2 mM KH_2PO_4, 10 mM Na_2HPO_4, 137 mM NaCl, 2.7 mM KCl) pH 7.4, 1 mM DTT, 37% glycerol and stored at −20 °C. Control proteins GCN4-pIqI, Acid-a1 and Base-a1 (see below) were designed with *E. coli* optimized codons using DNA Works,[46] gene synthesized by PCR, ligated into the pENTR vector using D-TOPO cloning, recombined into the pMAL derivative expression vector, and purified as above.

Cys-containing MBP-SYNZIP-His6X proteins were labeled using maleimide chemistry with fluorescein-5-maleimide (N-terminal or C-terminal) or Rhodamine Red C2 maleimide (N-terminal only) (Invitrogen). A 50 pmol portion of protein from glycerol stocks was reduced with 1 mM TCEP-HCl (Pierce) and then buffer exchanged into degassed PBS. The fluorophore was added at 10-fold molar excess and incubated at room temperature overnight with rotation. After labeling, free dye was removed by a desalting spin column (Pierce), followed by an additional amylose (NEB) and then NiNTA (Qiagen) column purification. Efficiently labeled protein yielded an ∼1:1 ratio of fluorophore to protein concentration for a sample, based on measuring the absorbance at 495 nm (fluorescein, ε = 68,000 M^{-1} c^{-1}, Thermo Scientific instruction bulletin 0359.2) or 573 nm (rhodamine, ε = 119,000 M^{-1} c^{-1}, Molecular Probes Handbook, 11th edition) in PBS for the dye and 280 nm in 6 M guanidine HCl for the protein. We ensured the applicability of this metric by testing several samples using analytical HPLC, indicating free dye had been eliminated and a single population of labeled protein remained.

Size-Exclusion Chromatography (SEC) Assay. Unlabeled MBP-SYNZIP proteins were prepared either alone at 10 μM or in pairs at 10 μM each in PBS pH 7.4, 1 mM DTT. Mixtures were either incubated at room temperature for 2 h or, for those mixtures with a partner that exhibited homo-oligomerization, incubated overnight at 37 °C and then cooled to room temperature for 2 h. Samples (50 μL) were run on a Waters HPLC system over a Superdex 75 10/300 column (GE Healthcare) at a flow rate of 0.5 mL/min in PBS pH 7.4, 1 mM DTT while monitoring absorbance at 215 nm. Empower software (Waters) was used to analyze the elution profiles. A

trimer control was based on the homotrimeric GCN4-pIqI protein,[35] with the sequence RMKQIEDKIEEILSKQYHIENEIARIKKLIGER, which was cloned into the MBP destination vector described above.

Fluorescence Resonance Energy Transfer (FRET) Assay. The fluorescence emission of N- and C-terminally fluorescein-labeled constructs was measured alone and, when mixed with N-terminally rhodamine-labeled partner, in triplicate. Samples (100 μL) were mixed at 100 nM concentration of each protein in PBS pH 7.4, 1 mM DTT, allowed to incubate 2 h at 37 °C, and then equilibrated 1 h at room temperature. Samples were excited at 480 nm, and emission at 525 nm was monitored at 25 °C. Protein concentrations were determined by the absorbance of the attached fluorophore in PBS pH 7.4, 1 mM DTT using an extinction coefficient of 68,000 cm^{-1} M^{-1} for fluorescein and 119,000 cm^{-1} M^{-1} for rhodamine. Samples were assayed in 384-well black plates (Corning) using a SpectraMax M5 plate reader (Molecular Devices). The FRET efficiency was calculated from the average of three samples as

$$\text{FRET efficiency} = 1 - \frac{\text{emission}_{\text{mix}}}{\text{emission}_{\text{donor}}}$$

Equilibration of the peptide mixtures was assessed by remeasuring plates after overnight incubation at 4 °C and re-equilibration at room temperature for 1 h, which gave no appreciable change in FRET efficiencies. The antiparallel heterodimerizing proteins[34] Acid-a1 (AQLEKELQALEKELAQLEWENQALEKELAQ), and Base-a1 (AQLKKKLQANKKKLAQLKWKLQALKKKLAQ) were cloned into the MBP destination vector described above and used as controls.

Fluorescence Polarization (FP) Assay. MBP-SYNZIP fluoresceinated proteins at 10 nM were mixed with unlabeled MBP-SYNZIPs at concentrations ranging from 60 pM to 20 μM, depending on the affinity range of the interaction, in PBS pH 7.4, 1 mM DTT in 384 well black plates (Corning), at a total volume of 100 μL. The concentrations of all proteins were determined by measuring absorbance at 280 nm in 6 M guanidine HCl. Samples were incubated at 37 °C for 2 h and then allowed to equilibrate at room temperature a minimum of 1 h. Polarization was monitored at 480/525 nm excitation/emission using a SpectraMax M5 plate reader (Molecular Devices) at 25 °C. Equilibration of the interactions was assessed by remeasuring plates after overnight incubation at 4 °C and re-equilibration at room temperature for 1 h, and no appreciable change in polarization signal was observed. For the FP competition assay, 20 nM labeled protein was mixed with each unlabeled partner at 1 μM, incubated at 37 °C for 2 h, and then equilibrated at room temperature for 1 h before being read as described above. Raw fluorescence of the labeled protein was also measured for each well to ensure a constant amount of labeled protein, and a small number of outliers were removed. Dissociation constants (K_d's) were determined by curve fitting using Excel. The average polarization of replicates was normalized to fraction bound (f_b) using the equation

$$f_b = \frac{S - S_{\min}}{S_{\max} - S_{\min}}$$

where S is the measured signal, $S_{\min}$ is the signal of the lower baseline, and $S_{\max}$ the upper baseline, selected on the basis of best fit after multiple curve fitting analyses of the data. Binding curves were then fit to the equation

$$f_b = \frac{(K_d + L_0 + P_0)^2 - 4L_0P_0}{2L_0}$$

where K_d is the dissociation constant, P_0 is the initial concentration of the unlabeled protein, and L_0 is the initial concentration of labeled protein. K_d values were fit using nonlinear least-squares and the Solver plug-in for Excel. In some cases, the initial fit of the curves to the data was poor, but fits assuming a lower concentration of the labeled species gave dramatic improvements. Because of the potential for nonspecific binding of the labeled species to the plastic used in the assay, it is realistic that the labeled probe concentration might be lower than 10 nM. Thus, in cases where the fit poorly matched the data, we fit both the K_d and the labeled species concentration (within the range 1−10 nM), and in all cases a lower concentration of labeled species improved the fit to the data significantly.

Yeast Two-Hybrid Assay. The interaction of SYNZIP pairs was tested using the ProQuest two-hybrid system (Invitrogen), in which an interaction reconstitutes Gal4 activity and drives *HIS3* and *URA3* expression, allowing identification of interactions based on growth on selective media.[36,37,47] SYNZIPs fused to the Gal4 activation domain (ADSZs) were transformed into the yeast strain MaV103; SYNZIPs fused to the DNA-binding domain of Gal4 (DBDSZs) were transformed into the strain MaV203 (both strains a gift of M. Vidal). Two liquid cultures inoculated from single colonies were independently grown overnight at 30 °C, aliquoted into 96-well plates, mixed with interaction partners in duplicate from the opposite mating type, and pin stamped onto YPD plates, resulting in four replicates in total. After overnight growth at 30 °C, colonies were replica plated onto synthetic complete media lacking leucine and tryptophan, to select for yeast carrying both plasmids, and incubated at 30 °C. Liquid cultures were then grown overnight, aliquoted into 96-well plates, and pin stamped onto synthetic complete media either without uracil (high stringency) or without histidine and with increasing concentrations of 3-AT (Sigma) from 10 to 100 mM (low to high stringency), as well as selection for plasmid maintenance. Autoactivation controls for both ADSZs and DBDSZs were performed using the same method without the mating step, with plating on appropriate dropout media. Colony size was imaged after 12 days for growth without uracil (-ura) and without histidine supplemented with 100 mM 3-AT (-his). CellProfiler[48] was used to determine the area of the colonies, and analysis of processed image data was performed in Matlab.

To compare the two-hybrid data to the published coiled-coil array data and to summarize the differences graphically, we symmetrized the yeast data by taking the stronger of the two observed interaction signals for pairs that were tested reciprocally. We binned the 253 resulting pairs into those that showed strong growth (59 pairs -his, 37 -ura), no growth (174 pairs -his, 187 -ura), or medium/indeterminate growth (14 pairs -his, 23 -ura). The indeterminate pairs, as well as 6 additional pairs that involved interactions between two autoactivators, were excluded from further analyses. The array results were processed using *arrayscores* reported by Reinke *et al.*,[30] where low scores indicate strong interactions. For the analysis reported in the text we used a cutoff of *arrayscore* < 0.6 to identify high-confidence array interactions. A less strict cutoff

of *arrayscore* < 0.75 also gives good agreement with the yeast data.

MAPK Pathway Testing. MAPK pathway testing followed the protocol described by Bashor *et al.*[9] Msg5-SYNZIP fusions were integrated into the *LEU2* locus of the yeast strain CB011 using a pRS305-derivative vector and expressed with a constitutive moderate strength promoter from *CYC1*. These strains were then transformed a second time with Ste5-SYNZIPs expressed on a CEN/ARS low copy number pRS316-derived plasmid driven by the *STE5* promoter. Liquid cultures of dual transformants were grown overnight and then diluted and grown to an OD_{600} of ~0.6. Cultures were treated with 2 μM α-factor, and expression was stopped at 120 min with cycloheximide at 5 μg/mL. The GFP reporter was allowed to mature at room temperature for 1 h, and then the mean cell fluorescence of populations of approximately 10,000 cells was measured on an LSR II FACS equipped with a high-throughput sampler using FACSDIVA software (BD Biosciences) followed by data analysis using FlowJo software (Treestar Inc.). For each interaction tested, measurements were done in quadruplicate by picking four initial colonies into separate cultures and performing the assay for each culture. Because of variability in the overall scale of the fluorescence signals between days and strains, signals were corrected for the pre-induction baseline and also normalized using results for strains with no SYNZIP fused to Msg5. The following formula was applied

$$S_n = \frac{S_{\text{ind}} - S_{\text{basal}}}{S_{\text{ind.noSZ}} - S_{\text{basal.noSZ}}}$$

where S_{ind} is the mean cell fluorescence after 2-h α-factor induction, S_{basal} is mean cell fluorescence before α-factor induction, and $S_{\text{ind\_noSZ}}$ and $S_{\text{basal\_noSZ}}$ are the corresponding post- and pre-induction signals for strains harboring the appropriate Ste5-SYNZIP along with Msg5 without a SYNZIP fusion.

■ ASSOCIATED CONTENT

Supporting Information

Specification sheets, documents, and spreadsheets. This material is available free of charge *via* the Internet at http://pubs.acs.org.

■ AUTHOR INFORMATION

Corresponding Author

*E-mail: keating@mit.edu.

Present Address

[‖]Howard Hughes Medical Institute, Department of Biomedical Engineering, Center for BioDynamics and Center for Advanced Biotechnology, Boston University, Boston, Massachusetts 02215, USA.

Author Contributions

K.E.T., C.J.B., W.A.L., and A.E.K. designed the experiments and analyzed the data. K.E.T. and C.J.B. performed the experiments. K.E.T. and A.E.K. wrote the paper.

Notes

The authors declare no competing financial interest.

■ ACKNOWLEDGMENTS

We thank N. Zizlsperger, R. Goodman, R. Neupane, and K. Zhang for help with experiments, K. Hauschild for advice and input on many aspects of the project and members of the Keating lab for comments on the work and the manuscript. We also thank Marc Vidal and David Hill for the yeast two-hybrid strains. K.E.T. and A.E.K. were supported by NSF award MCB 0950233. C.J.B. and W.A.L. were supported by National Institutes of Health grants RO1 GM55040, PN2 EY016546, and P50 GMO81879, the NSF Synthetic Biology Engineering Research Center, and the Howard Hughes Medical Institute.

■ REFERENCES

(1) Canton, B., Labno, A., and Endy, D. (2008) Refinement and standardization of synthetic biological parts and devices. *Nat. Biotechnol. 26*, 787−793.

(2) Kelly, J. R., Rubin, A. J., Davis, J. H., Ajo-Franklin, C. M., Cumbers, J., Czar, M. J., de Mora, K., Glieberman, A. L., Monie, D. D., and Endy, D. (2009) Measuring the activity of BioBrick promoters using an in vivo reference standard. *J. Biol. Eng. 3*, 4.

(3) Davis, J. H., Rubin, A. J., and Sauer, R. T. (2011) Design, construction and characterization of a set of insulated bacterial promoters. *Nucleic Acids Res. 39*, 1131−1141.

(4) Babiskin, A. H., and Smolke, C. D. (2011) A synthetic library of RNA control modules for predictable tuning of gene expression in yeast. *Mol. Syst. Biol. 7*, 471.

(5) Salis, H. M., Mirsky, E. A., and Voigt, C. A. (2009) Automated design of synthetic ribosome binding sites to control protein expression. *Nat. Biotechnol. 27*, 946−950.

(6) Tamsir, A., Tabor, J. J., and Voigt, C. A. (2011) Robust multicellular computing using genetically encoded NOR gates and chemical 'wires'. *Nature 469*, 212−215.

(7) Lee, T. S., Krupa, R. A., Zhang, F., Hajimorad, M., Holtz, W. J., Prasad, N., Lee, S. K., and Keasling, J. D. (2011) BglBrick vectors and datasheets; a synthetic biology platform for gene expression. *J. Biol. Eng. 5*, 12.

(8) Wang, B., Kitney, R. I., Joly, N., and Buck, M. (2011) Engineering modular and orthogonal genetic logic gates for robust digital-like synthetic biology. *Nat. Commun. 2*, 508.

(9) Bashor, C. J., Helman, N. C., Yan, S., and Lim, W. A. (2008) Using engineered scaffold interactions to reshape MAP kinase pathway signaling dynamics. *Science 319*, 1539−1543.

(10) Dueber, J. E., Wu, G. C., Malmirchegini, G. R., Moon, T. S., Petzold, C. J., Ullal, A. V., Prather, K. L., and Keasling, J. D. (2009) Synthetic protein scaffolds provide modular control over metabolic flux. *Nat. Biotechnol. 27*, 753−759.

(11) Moon, T. S., Dueber, J. E., Shiue, E., and Prather, K. L. (2010) Use of modular, synthetic scaffolds for improved production of glucaric acid in engineered E. coli. *Metab. Eng. 12*, 298−305.

(12) Lumb, K. J., Carr, C. M., and Kim, P. S. (1994) Subdomain folding of the coiled coil leucine zipper from the bZIP transcriptional activator GCN4. *Biochemistry 33*, 7361−7367.

(13) Mason, J. M., Muller, K. M., and Arndt, K. M. (2007) Considerations in the design and optimization of coiled coil structures. *Methods Mol. Biol. 352*, 35−70.

(14) Acharya, A., Rishi, V., and Vinson, C. R. (2006) Stability of 100 homo and heterotypic coiled-coil a-a' pairs for ten amino acids (A, L, I, V, N, K, S, T, E, and R). *Biochemistry 45*, 11324−11332.

(15) Acharya, A., Ruvinov, S. B., Gal, J., Moll, J. R., and Vinson, C. R. (2002) A heterodimerizing leucine zipper coiled coil system for examining the specificity of a position interactions: amino acids I, V, L, N, A, and K. *Biochemistry 41*, 14122−14131.

(16) Chattopadhyay, K., Ramagopal, U. A., Mukhopadhaya, A., Malashkevich, V. N., Dilorenzo, T. P., Brenowitz, M., Nathenson, S. G., and Almo, S. C. (2007) Assembly and structural properties of glucocorticoid-induced TNF receptor ligand: Implications for function. *Proc. Natl. Acad. Sci. U.S.A. 104*, 19452−19457.

(17) Eckert, D. M., Malashkevich, V. N., Hong, L. H., Carr, P. A., and Kim, P. S. (1999) Inhibiting HIV-1 entry: discovery of D-peptide inhibitors that target the gp41 coiled-coil pocket. *Cell 99*, 103−115.

(18) Strelkov, S. V., Herrmann, H., Geisler, N., Wedig, T., Zimbelmann, R., Aebi, U., and Burkhard, P. (2002) Conserved

segments 1A and 2B of the intermediate filament dimer: their atomic structures and role in filament assembly. *EMBO J. 21*, 1255−1266.
(19) Weissenhorn, W., Carfi, A., Lee, K. H., Skehel, J. J., and Wiley, D. C. (1998) Crystal structure of the Ebola virus membrane fusion subunit, GP2, from the envelope glycoprotein ectodomain. *Mol. Cell 2*, 605−616.
(20) Weissenhorn, W., Dessen, A., Harrison, S. C., Skehel, J. J., and Wiley, D. C. (1997) Atomic structure of the ectodomain from HIV-1 gp41. *Nature 387*, 426−430.
(21) Gribbon, C., Channon, K. J., Zhang, W., Banwell, E. F., Bromley, E. H., Chaudhuri, J. B., Oreffo, R. O., and Woolfson, D. N. (2008) MagicWand: a single, designed peptide that assembles to stable, ordered alpha-helical fibers. *Biochemistry 47*, 10365−10371.
(22) Wolfe, S. A., Grant, R. A., and Pabo, C. O. (2003) Structure of a designed dimeric zinc finger protein bound to DNA. *Biochemistry 42*, 13401−13409.
(23) Wolfe, S. A., Ramm, E. I., and Pabo, C. O. (2000) Combining structure-based design with phage display to create new Cys(2)His(2) zinc finger dimers. *Structure 8*, 739−750.
(24) Mapp, A. K., Ansari, A. Z., Ptashne, M., and Dervan, P. B. (2000) Activation of gene expression by small molecule transcription factors. *Proc. Natl. Acad. Sci. U.S.A. 97*, 3930−3935.
(25) Holmström, S. C., King, P. J., Ryadnov, M. G., Butler, M. F., Mann, S., and Woolfson, D. N. (2008) Templating silica nanostructures on rationally designed self-assembled peptide fibers. *Langmuir 24*, 11778−11783.
(26) Papapostolou, D., Bromley, E. H., Bano, C., and Woolfson, D. N. (2008) Electrostatic control of thickness and stiffness in a designed protein fiber. *J. Am. Chem. Soc. 130*, 5124−5130.
(27) Papapostolou, D., Smith, A. M., Atkins, E. D., Oliver, S. J., Ryadnov, M. G., Serpell, L. C., and Woolfson, D. N. (2007) Engineering nanoscale order into a designed protein fiber. *Proc. Nat.l Acad. Sci. U.S.A. 104*, 10853−10858.
(28) Ryadnov, M. G., Ceyhan, B., Niemeyer, C. M., and Woolfson, D. N. (2003) "Belt and braces": a peptide-based linker system of de novo design. *J. Am. Chem. Soc. 125*, 9388−9394.
(29) Shen, W., Zhang, K., Kornfield, J. A., and Tirrell, D. A. (2006) Tuning the erosion rate of artificial protein hydrogels through control of network topology. *Nat. Mater. 5*, 153−158.
(30) Reinke, A. W., Grant, R. A., and Keating, A. E. (2010) A synthetic coiled-coil interactome provides heterospecific modules for molecular engineering. *J. Am. Chem. Soc. 132*, 6025−6031.
(31) Grigoryan, G., Reinke, A. W., and Keating, A. E. (2009) Design of protein-interaction specificity gives selective bZIP-binding peptides. *Nature 458*, 859−864.
(32) Grigoryan, G., and Keating, A. E. (2008) Structural specificity in coiled-coil interactions. *Curr. Opin. Struct. Biol. 18*, 477−483.
(33) Harbury, P. B., Zhang, T., Kim, P. S., and Alber, T. (1993) A switch between two-, three-, and four-stranded coiled coils in GCN4 leucine zipper mutants. *Science 262*, 1401−1407.
(34) Oakley, M. G., and Kim, P. S. (1998) A buried polar interaction can direct the relative orientation of helices in a coiled coil. *Biochemistry 37*, 12603−12610.
(35) Eckert, D. M., Malashkevich, V. N., and Kim, P. S. (1998) Crystal structure of GCN4-pIQI, a trimeric coiled coil with buried polar residues. *J. Mol. Biol. 284*, 859−865.
(36) Chevray, P. M., and Nathans, D. (1992) Protein interaction cloning in yeast: identification of mammalian proteins that react with the leucine zipper of Jun. *Proc. Natl. Acad. Sci. U.S.A. 89*, 5789−5793.
(37) Vidal, M., Brachmann, R. K., Fattaey, A., Harlow, E., and Boeke, J. D. (1996) Reverse two-hybrid and one-hybrid systems to detect dissociation of protein-protein and DNA-protein interactions. *Proc. Natl. Acad. Sci. U.S.A. 93*, 10315−10320.
(38) Boxem, M., Maliga, Z., Klitgord, N., Li, N., Lemmens, I., Mana, M., de Lichtervelde, L., Mul, J. D., van de Peut, D., Devos, M., Simonis, N., Yildirim, M. A., Cokol, M., Kao, H. L., de Smet, A. S., Wang, H. D., Schlaitz, A. L., Hao, T., Milstein, S., Fan, C. Y., Tipsword, M., Drew, K., Galli, M., Rhrissorrakrai, K., Drechsel, D., Koller, D., Roth, F. P., Iakoucheva, L. M., Dunker, A. K., Bonneau, R., Gunsalus, K. C., Hill, D. E., Piano, F., Tavernier, J., van den Heuvel, S., Hyman, A. A., and Vidal, M. (2008) A protein domain-based interactome network for C-elegans early embryogenesis. *Cell 134*, 534−545.
(39) Yu, H., Braun, P., Yildirim, M. A., Lemmens, I., Venkatesan, K., Sahalie, J., Hirozane-Kishikawa, T., Gebreab, F., Li, N., Simonis, N., Hao, T., Rual, J. F., Dricot, A., Vazquez, A., Murray, R. R., Simon, C., Tardivo, L., Tam, S., Svrzikapa, N., Fan, C., de Smet, A. S., Motyl, A., Hudson, M. E., Park, J., Xin, X., Cusick, M. E., Moore, T., Boone, C., Snyder, M., Roth, F. P., Barabasi, A. L., Tavernier, J., Hill, D. E., and Vidal, M. (2008) High-quality binary protein interaction map of the yeast interactome network. *Science 322*, 104−110.
(40) Vinson, C. R., Acharya, A., and Taparowsky, E. J. (2006) Deciphering B-ZIP transcription factor interactions in vitro and in vivo. *Biochim. Biophys. Acta 1759*, 4−12.
(41) Smoot, M. E., Ono, K., Ruscheinski, J., Wang, P. L., and Ideker, T. (2011) Cytoscape 2.8: new features for data integration and network visualization. *Bioinformatics 27*, 431−432.
(42) Grunberg, R., Ferrar, T. S., van der Sloot, A. M., Constante, M., and Serrano, L. (2010) Building blocks for protein interaction devices. *Nucleic Acids Res. 38*, 2645−2662.
(43) Kohler, J. J., and Schepartz, A. (2001) Kinetic studies of Fos.Jun.DNA complex formation: DNA binding prior to dimerization. *Biochemistry 40*, 130−142.
(44) Chao, H., Houston, M. E. Jr., Grothe, S., Kay, C. M., O'Connor-McCourt, M., Irvin, R. T., and Hodges, R. S. (1996) Kinetic study on the formation of a de novo designed heterodimeric coiled-coil: use of surface plasmon resonance to monitor the association and dissociation of polypeptide chains. *Biochemistry 35*, 12175−12185.
(45) Villalobos, A., Ness, J. E., Gustafsson, C., Minshull, J., and Govindarajan, S. (2006) Gene Designer: a synthetic biology tool for constructing artificial DNA segments. *BMC Bioinf. 7*, 285.
(46) Hoover, D. M., and Lubkowski, J. (2002) DNAWorks: an automated method for designing oligonucleotides for PCR-based gene synthesis. *Nucleic Acids Res. 30*, e43.
(47) Vidal, M. (1997) The reverse two-hybrid system, in *The Yeast Two-Hybrid System* (Bartel, P., and Fields, S., Eds.), pp 109−147, Oxford University Press, New York, NY.
(48) Lamprecht, M. R., Sabatini, D. M., and Carpenter, A. E. (2007) CellProfiler: free, versatile software for automated biological image analysis. *Biotechniques 42*, 71−75.